

Effect of disorder in the charge-density-wave compounds $\text{LaTe}_{1.95}$ and $\text{CeTe}_{1.95-x}\text{Se}_x$ ($x=0$ and 0.16) as revealed by optical spectroscopy

Y. Huang, B. F. Hu, T. Dong, A. F. Fang, P. Zheng, and N. L. Wang
*Beijing National Laboratory for Condensed Matter Physics, Institute of Physics,
 Chinese Academy of Sciences, Beijing 100190, People's Republic of China*

We present optical spectroscopy measurements on rare-earth ditelluride single crystals of $\text{LaTe}_{1.95}$ and $\text{CeTe}_{1.95-x}\text{Se}_x$ ($x=0$ and 0.16). The measurements reveal formation of charge density wave energy gaps at rather high energy levels, e.g. $2\Delta \sim 8500 \text{ cm}^{-1}$ for $\text{LaTe}_{1.95}$, and 6800 cm^{-1} for $\text{CeTe}_{1.95}$. More strikingly, the study reveals that, different from the rare-earth tri-tellurides, the Te vacancies and disorder effect play a key role in the low-energy charge excitations of ditelluride systems. Although an eminent peak is observed between 800 and 1500 cm^{-1} in conductivity spectra for $\text{LaTe}_{1.95}$, and $\text{CeTe}_{1.95-x}\text{Se}_x$ ($x=0, 0.16$), our analysis indicates that it could not be attributed to the formation of a small energy gap, instead it could be well accounted for by the localization modified Drude model. Our study also indicates that the low-temperature optical spectroscopic features are distinctly different from a semiconducting CDW state with entirely gapped Fermi surfaces.

PACS numbers: 71.45.Lr, 78.20.-e, 78.30.Er

I. INTRODUCTION

Charge density wave (CDW) is a collective quantum phenomenon in solids and a subject of considerable interest in condensed matter physics. Most CDW states are driven by the nesting topology of Fermi surface (FS), i.e. the matching of sections of FS to others by a wave vector $2\mathbf{k}_F$, where the electronic susceptibility has a divergence. A single particle energy gap opens in the nested regions of the Fermi surfaces at the transition, which leads to the lowering of the electronic energies of the system. Coupling to the lattice, the development of CDW state would also cause a lattice distortion with the modulation wave vector of superstructure matching with the FS nesting wave vector.¹

The nesting condition is easily realized in low-dimensional electronic systems. In one-dimensional (1D) CDW systems, a perfect nesting can be realized and the FS could be fully gapped. Then the systems become insulating or semiconducting in the CDW phase. For 2D or 3D CDW systems, a perfect nesting of the entire FSs could hardly be fulfilled. In this circumstance, the CDW energy gap forms only on the partially nested region of FSs. Due to the presence of ungapped region of FSs, the system would remain metallic even in the CDW state.

The rare-earth polychalcogenides RTe_n (where R is La or rare earth element, $n=2, 2.5, 3$) are prototype CDW-bearing materials. These systems have layered structures, consisting of corrugated rare-earth-chalcogen slabs alternated with planar chalcogen Te square lattice. R in the compound is trivalent, donating three electrons to the system. They completely fill the Te p orbitals in the RTe slabs, but partially those Te p orbitals in the square Te-layers^{2,3}. Metallic conduction occurs in the Te layers, leading to highly anisotropic transport properties^{2,4,5}. Nested regions of FSs were indicated by both band structure calculations and ARPES measurements⁶⁻⁹, which has been well characterized as the origin of CDW formation. Pressure-induced superconductivity was also found in several systems of both rare-earth tri- and di-tellurides in the family^{10,11}, yielding good candidates for investigating

the competition between superconductivity and CDW orders. Among the family, the rare-earth tri-telluride RTe_3 , which consists of double Te layers between insulating corrugated RTe slabs, were widely studied. Two energy gaps with different energy scales were observed^{12,13}, which were considered as driven by two different nesting wave vectors present in the FS topology. Similar to other 2D CDW systems, the ungapped regions of FSs are always present in RTe_3 and the materials remain metallic in CDW state. Compared with rare-earth tri-telluride RTe_3 , much less work has been done on the rare-earth ditelluride RTe_2 which consists of single Te layers between insulating corrugated RTe slab (see inset of Fig. 1). The reported CDW gap structures by ARPES measurement are rather controversial. Shin *et al.* performed ARPES measurements on $\text{LaTe}_{1.95}$ and CeTe_2 and found that for both compounds the inner FSs center at Γ point are almost fully gapped with $E_g=600 \text{ meV}$ while the outer FSs are only partially gapped with $E_g=100 \text{ meV}$.⁹ On the other hand, Garcia *et al.* investigated LaTe_2 compound and found that the entire inner and outer FSs are gapped by a surprisingly small energy scale of $E_g=50 \text{ meV}$ as determined from the leading edge shift¹⁴. They claimed that CDW gap size decreases dramatically as the number of the Te layers reduces from two (RTe_3) to one (RTe_2) and the LaTe_2 would be the first proven instance of semiconducting quasi-2D CDW material¹⁴.

It would be essential to clarify the issue by performing different spectroscopic measurements. It should be noted that, unlike the case of rare-earth tri-tellurides where the conducting Te layers are free from defects, Te vacancies in Te layers were found to be present in most reported work on rare-earth ditelluride RTe_2 compounds. Special care has to be taken on the sample characterizations. Optical spectroscopy is a powerful bulk sensitive technique to detect the energy gaps in ordered state and yields a great wealth of information in CDW systems. Here we present optical spectroscopic measurements on $\text{LaTe}_{1.95}$, pure and Se-doped $\text{CeTe}_{1.95}$ single crystals. Our measurement indicates clearly the formation of CDW gap structure at rather high energy level with $2\Delta \sim 8500 \text{ cm}^{-1}$ ($\sim 1.06 \text{ eV}$) for $\text{LaTe}_{1.95}$. The energy scale of the CDW gap is gradually reduced for the pure and Se-doped

CeTe_{1.95} samples. Although a pronounced peak at low energy scale, between 800~1500 cm⁻¹ (0.1~0.2 eV) for LaTe_{1.95} and CeTe_{1.95-x}Se_x (x=0, 0.16), is also observed, our study suggests that the low energy excitations are dominantly contributed by the disorder effects due to the presence of Te vacancies in Te layers. The experimental results are very different from the defect-free rare-earth tritelluride RTe₃ compounds where small CDW energy gaps could be clearly indicated. Furthermore, the spectral features are distinctly different from a semiconducting CDW state with fully gapped Fermi surfaces.

II. EXPERIMENT AND RESULTS

Single crystals of RTe_{2-x} (R=La, Ce) have been grown by a self-flux technique.⁹ The mixtures of rare-earth powders and Te pieces in an atomic ratio from 0.16:0.84 to 0.18:0.82 were placed in an alumina crucible and sealed in an evacuated quartz tube. The mixture was heated up to 1150°C and kept for one day, then cooled down slowly to 1000°C over a period of 5 days. At the final temperature, the rest flux Te was separated from single crystals in a centrifuge. Shiny and dark colored crystals were obtained. The crystals were found to be air- and moisture-sensitive. We also grew Se-doped single crystals of CeTe₂ from similar process by changing the starting compositions to Ce_{0.18}Te_{0.76}Se_{0.06}.

Figure 1 displays the X-ray diffraction pattern of CeTe_{2-x} single crystals at room temperature. The (0 0 *l*) diffraction peaks indicate a good c-axis characteristic. The obtained c-axis lattice parameter is *c*=9.11, which agrees well with the previous result.¹⁵ The energy dispersive X-ray spectroscopy (EDX) analysis equipped with the scanning electron microscope (SEM) indicates that both the La- and Ce-based compounds have average compositions of R:Te≈1:1.95 (R=La, Ce). The Se-doped crystal has an average composition of CeTe_{1.79}Se_{0.16}. Obviously, Te deficiencies are present in the crystals although the self-flux method was reported to be effective on reducing the Te vacancies.⁹ As we shall elaborate in this work, those Te vacancies greatly affect the optical properties of RTe₂ systems.

The temperature dependence of the in-plane (ac-plane) dc conductivity $\rho(T)$ was measured by a standard four-probe method in a quantum design physical properties measurement system (PPMS) and plotted in Fig. 2. Platinum wires were fixed on the sample using highly conducting silver adhesive in the glove-box to avoid deterioration. The resistivity of both CeTe_{1.95} and LaTe_{1.95} shows metallic behavior with relatively high absolute values at base temperature in comparison with RTe₃. In an earlier report by Shin et al.⁹, the resistivity of LaTe_{1.95} shows an upturn at low temperature. The different behaviors could be attributed to slightly different sample quality. Due to Te deficiencies, $\rho(T)$ values change between crystals^{9,16}. In addition, CeTe_{1.95} compound shows a sharp feature at about 5K, which is related to the anti-ferromagnetic ordering of spins from the localized 4f electrons of Ce. On the other hand, the resistivity behavior is rather different when Te was partially substituted by

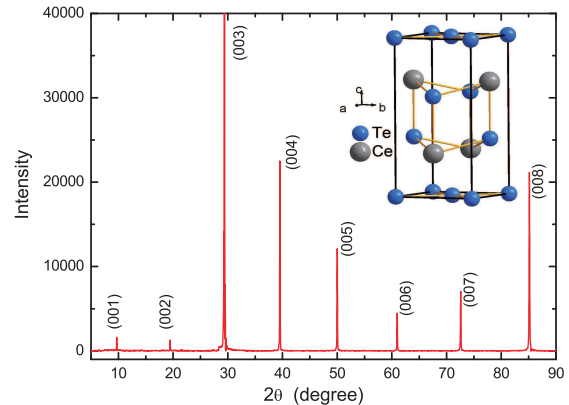


FIG. 1: (Color online) The (00*l*) x-ray diffraction pattern of single-crystal CeTe_{1.95}. The strongest peak is only partially displayed in order to show others clearly. The inset shows the crystal structure.

Se. The resistivity of CeTe_{1.95-x}Se_x (x=0.16) increases modestly with decreasing temperature. An anomaly is surprisingly seen near 345 K both in cooling and warming processes. We performed transmission electron microscopy (TEM) measurement on this sample and found that the superlattice diffraction spots disappear at temperatures above 345 K. Combined with the results from optical study below, we believe that it could be ascribed to CDW phase transition.

The optical reflectivity measurement was carried out on Bruker IFS 113v and 80v/s spectrometers in a frequency range from 40 to 25000 cm⁻¹. An *in situ* gold and aluminium overcoating technique was used to get the reflectivity $R(\omega)$. Kramers-Kronig transformation of $R(\omega)$ is employed to get the real part of the conductivity spectra $\sigma_1(\omega)$. A Hagen-

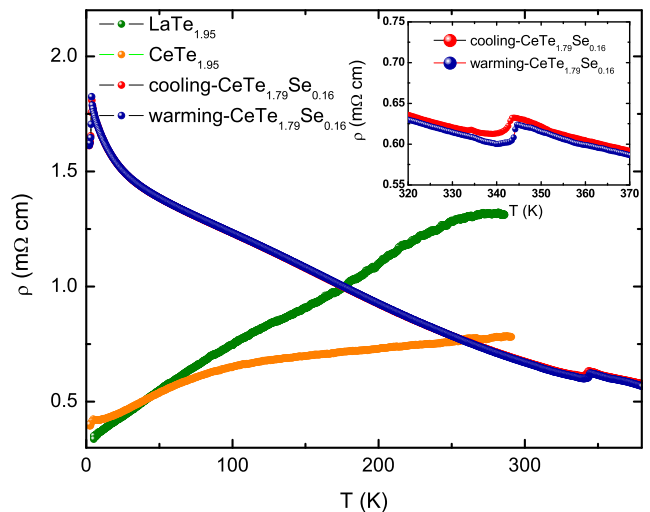


FIG. 2: (Color online) The temperature dependent in-plane (ac-plane) resistivity, showing LaTe_{1.95}, CeTe_{1.95} and CeTe_{1.79}Se_{0.16}. Inset: the details of the anomaly of CeTe_{1.79}Se_{0.16} between 340k and 350k.

Rubens relation was used for the low frequency extrapolation. A constant value of high frequency extrapolation was used up to 100000 cm^{-1} , above which an ω^{-4} relation was employed.

Figure 3 show the optical reflectance $R(\omega)$ and real part of conductivity $\sigma_1(\omega)$ of $\text{LaTe}_{1.95}$, $\text{CeTe}_{1.95-x}\text{Se}_x$ ($x=0$ and 0.16), respectively. The insets of upper panels show $R(\omega)$ in the expanded rang up to 25000 cm^{-1} . The $R(\omega)$ of the those compounds have high values at low frequency and decreases rapidly with increasing frequency, forming plasma edges near 18000 cm^{-1} . The experimental results demonstrate that the materials are metallic even in the deep CDW state, consistent with the dc resistivity measurements.

Two significant features exist in the optical spectra of those samples. The first one is the very strong dip structure in $R(\omega)$ in the near infrared region $\sim 5000 \text{ cm}^{-1}$, which becomes more pronounced upon cooling. This leads to a remarkable peak structure in the conductivity spectra $\sigma_1(\omega)$ at higher energy scale. For the three samples, the conductivity peak is the most prominent for the $\text{LaTe}_{1.95}$ crystal. It locates near 8000 cm^{-1} at 300 K , and shifts to further higher energy scale $\sim 8500 \text{ cm}^{-1}$ as the temperature decreases to 10 K . For the pure and Se-doped $\text{CeTe}_{1.95}$ samples, the peak feature appears at lower energy scales and also becomes less pronounced. The spectra provide optical evidence for the presence of an energy gap, which could be ascribed to the CDW order. Because of the "type-I coherent factor" for density wave order which gives rise to a characteristic peak structure just above the energy gap in optical conductivity, the peak position in $\sigma_1(\omega)$ could be identified as the energy scale of CDW gap.^{17,18} The measurement results are in agreement with earlier reports.^{19,20} In ARPES measurements, the inner FSs centered at Γ point were found to be almost fully gapped with $E_g=600 \text{ meV}$ (roughly 4800 cm^{-1}) for $\text{LaTe}_{1.95}$.⁹ Since the ARPES measurement probes the gap relative to the Fermi level, while the optical measurement detects the excitation from occupied to unoccupied states, the gap value by optics should double the gap size probed by ARPES. Roughly, the gap values are consistent with earlier ARPES experiments.⁹ For the Se-doped $\text{CeTe}_{1.95-x}\text{Se}_x$ ($x=0.16$), since a resistivity jump is observed near 345 K , the CDW order is believed to be formed only below this temperature. Indeed, we found an absence of this gap feature in reflectance and conductivity spectra at measurement temperature 380 K .

The second very strong structure is the presence of another prominent peak in conductivity spectra $\sigma_1(\omega)$ at much lower energy scale, between $800\text{-}1500 \text{ cm}^{-1}$ for $\text{LaTe}_{1.95}$ and $\text{CeTe}_{1.95-x}\text{Se}_x$ ($x=0, 0.16$). This peak structure was also observed in earlier optical measurements and was assigned to an energy gap as well²⁰. Indeed, ARPES measurements revealed energy gap features roughly at the half of above values. Nevertheless, we noticed that the peak positions in $\sigma_1(\omega)$ moves slightly towards the lower energy as temperature decreases for those compounds. Such temperature dependent shift is opposite to the expectation of CDW energy gap formation. On this account, the low-energy peak structure could not be ascribed to the formation of a small CDW gap. This conclusion is further strengthened by the measurement on Se-doped $\text{CeTe}_{1.95-x}\text{Se}_x$ ($x=0.16$). For this sample, the CDW phase tran-

sition is already suppressed to 345 K . In accordance with this suppression, the energy gap feature near 6000 cm^{-1} is not visible in our optical measurement at 380 K . However, the low-energy peak feature is still present at all measurement temperatures. If the low-energy peak feature is developed from CDW order, it should be more easily suppressed by the Se doping. Considering the fact that the Te deficiencies are always present in the RTe_{2-x} samples and the conduction electrons are from the $5p$ electrons of square Te layers, we expect that the disorder-driven electron localization effect is the dominant contribution to the formation of the low-energy peak structure in $\sigma_1(\omega)$. It remains to be investigated whether or not the electron localization effect, which leads to the peak structure in $\sigma_1(\omega)$, could results in a gap-like feature in ARPES measurements. As we shall elaborate below, the localization modified Drude model could reasonably reproduce the spectral feature of the experimental data.

Besides the above two very strong spectral structures, we also noticed a weak feature near 10000 cm^{-1} in $R(\omega)$ for both $\text{LaTe}_{1.95}$ and $\text{CeTe}_{1.95}$ compounds, which is more clearly visible at low temperature and leads to a shoulder in $\sigma_1(\omega)$ spectra at slightly higher frequencies. Different from the notable shift of peak corresponding to CDW orders, the shoulder positions show little change at varied temperatures. It is likely that this feature comes from the inter-band transitions.

III. ANALYSIS FROM THE LOCALIZATION MODIFIED DRUDE MODEL

Let us now analyze the evolution of the itinerant carriers and the CDW gap excitations in a quantitative way. As stated above, we try to use the localization modified Drude (LMD) model, instead of a simple Drude term, to analyze the low frequency conductivity spectra, since the former is more appropriate in a carriers-localization system.²¹⁻²³ The high frequency interband transitions and energy gap excitations could be described by the Lorentz components. Within the LMD and Lorentz approach, the dielectric function would consist of two parts:

$$\epsilon(\omega) = \epsilon_{LMD}(\omega) + \sum_{i=1}^N \frac{S_i^2}{\omega_i^2 - \omega^2 - i\omega/\tau_i}. \quad (1)$$

and

$$\epsilon_{LMD}(\omega) = \epsilon_\infty - \frac{\omega_p^2}{\omega^2 + i\omega/\tau_D} \left[1 - \frac{C}{(k_F\lambda)^2} \left(\sqrt{\frac{3}{\omega\tau_D}} - (\sqrt{6} - 1) \right) \right]. \quad (2)$$

Here, the first term in expression (1) is the LMD component, the second term is the Lorents components. ϵ_∞ is the dielectric constant at high energy, ω_p the plasma frequency, k_F the Fermi wave vector, λ the mean free path and C a universal constant (~ 1). The model was found to reproduce the conductivity spectra fairly well. As examples, we show in Fig. 4 the experimental data together with the fitting curves for $\text{CeTe}_{1.95-x}\text{Se}_x$ ($x=0$ and 0.16) samples at 10 K , respectively. In Table 1 we list the fitting parameters for the three different

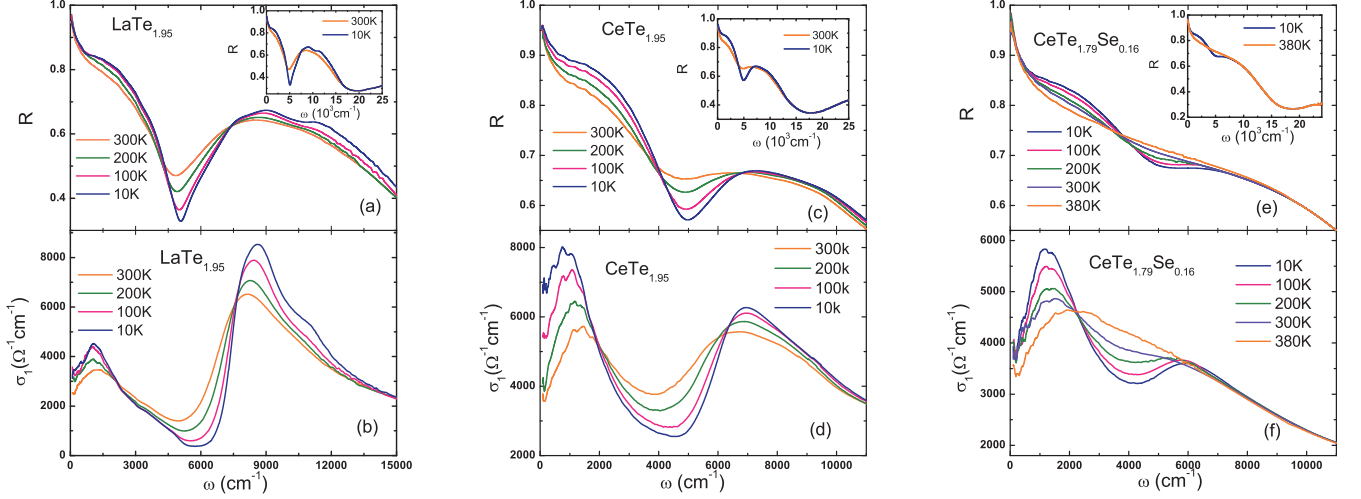


FIG. 3: (Color online) Left panel: (a) The temperature-dependence reflectivity of $\text{LaTe}_{1.95}$ below 15000 cm^{-1} . The inset shows the $R(\omega)$ at two representative temperatures up to 25000 cm^{-1} . (b) The frequency dependence of the real part of the conductivity at different temperatures. Inset: $\sigma_1(\omega)$ at 10 K and 300 K over a broad frequency range. Middle and right panels are for $\text{CeTe}_{1.95}$ and $\text{CeTe}_{1.79}\text{Se}_{0.16}$ respectively.

TABLE I: Temperature dependence of the plasma frequency ω_p , scattering rate $\gamma_D=1/\tau_D$ and order parameter $k_F\lambda$ of the LMD term, the resonance frequency ω_i , the width $\gamma_i=1/\tau_i$ and the square root of the oscillator strength S_i of the Lorentz component (all entries in 10^3 cm^{-1}). The Lorentz term in lowest energy responsible for the CDW order and the others responsible for inter-band transition.

Sample	ω_p	γ_D	$k_F\lambda$	ω_1	γ_1	S_1	ω_2	γ_2	S_2	ω_3	γ_3	S_3
$\text{LaTe}_{1.95}(10\text{K})$	21	1.5	1.3	8.5	2	27	10	5	30	23	40	60
$\text{LaTe}_{1.95}(300\text{K})$	21.3	2	1.07	8	2.5	24.7	10	5.3	29	23	40	60
$\text{CeTe}_{1.95}(10\text{K})$	26	1.3	1.18	6.8	2.4	22	8.8	5.6	29	22	40	65
$\text{CeTe}_{1.95}(300\text{K})$	27	2	1.12	6.2	3.4	21	8.3	5.7	28	22	40	65
$\text{CeTe}_{1.79}\text{Se}_{0.16}(10\text{K})$	23	1.6	0.9	6	3.2	14	9	14.7	36	-	-	-
$\text{CeTe}_{1.79}\text{Se}_{0.16}(380\text{K})$	34	4	1.14	-	-	-	9	19	32	-	-	-

samples at 300 (or 380) and 10 K, respectively. The disorder parameter ($k_F\lambda$) is in general greater than 1, which is in the metallic side of the metal-insulator transition in terms of Ioffe-Regel criterion. The model yields consistent values with the dc conductivity at the zero frequency limit where it takes the form for the metallic conduction,

$$\sigma_{LMD}(0) = \frac{\omega_p^2}{4\pi\gamma} \left[1 - \frac{1}{(k_F\lambda)^2} \right]. \quad (3)$$

This expression could account for the reduction of conductivity due to localization effect when $k_F\lambda > 1$.²⁴ Apparently, the LMD model is more suitable in describing the carrier response in the infrared region as it can account for the disorder effect presented in the samples. Nevertheless, it should be remarked that the ($k_F\lambda$) parameter becomes slightly smaller than 1 for $\text{CeTe}_{1.95-x}\text{Se}_x$ ($x=0.16$) sample at low temperature, indicating further enhanced localization effect. This effect could be naturally attributed to the random substitutions of Te sites by Se in the conducting Te layers, which drives the sample into the non-metallic side of the Ioffe-Regel criterion. The result is

consistent with the semiconducting dc resistivity behavior. In this circumstance, the LMD model is no longer valid for this sample.

The above analysis indicates that the free carrier response can be described by the LMD component. We found that ω_p of both $\text{LaTe}_{1.95}$ and $\text{CeTe}_{1.95}$ decreases very slightly from room temperature to 10K. On the other hand, the scattering rate ($\gamma = 1/\tau$) decreases even faster. However, for $\text{CeTe}_{1.95-x}\text{Se}_x$ ($x=0.16$), the plasma frequency $\omega_p = 33600 \text{ cm}^{-1}$ at 380 K reduces to 23000 cm^{-1} at 10 K. The square of plasma frequency ω_p is proportional to the effective carrier density n/m^* (where m^* is the effective carrier mass). This result could be interpreted as the formation of the partial CDW gap which removes those electrons near E_F that experience stronger scattering, leading to a reduction of both conducting carrier density and the scattering rate due to the reduction of scattering channels.

Our study indicates that the Te-vacancies or disorder effect play the key role in the low-energy charge excitations of rare-earth ditellurides RTe_{2-x} . This is different from the

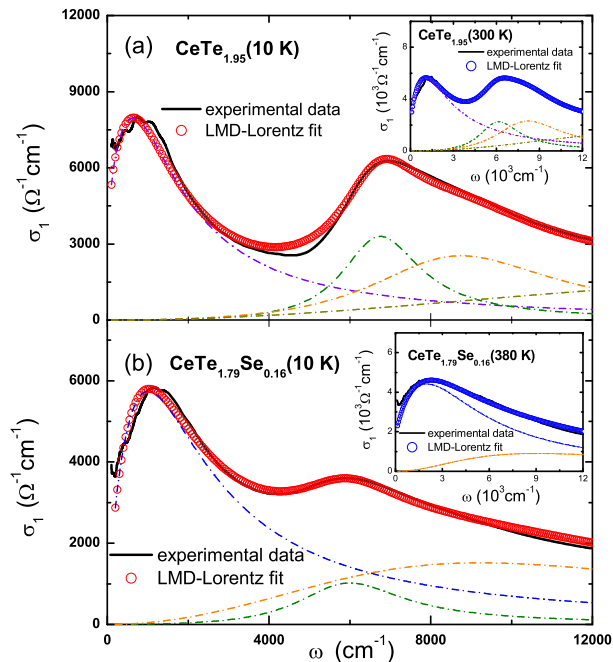


FIG. 4: (Color online) The experimental data of $\sigma_1(\omega)$ at 10 K and the LMD-Lorentz fit results for (a) $\text{CeTe}_{1.95}$ and (b) $\text{CeTe}_{1.79}\text{Se}_{0.16}$. The dashed curves displayed at the bottom in each panel are fitting components in the LMD-Lorentz analysis. The one at the lowest energy scale is the LMD component, the others at the higher energy scales are Lorentz components. Inset shows the corresponding results at 300 K or 380 K.

extensively investigated rare-earth tri-telluride RTe_3 where Te vacancies were usually not detected. We would also like to remark that the disorder effect could also dramatically affect the CDW phase transitions.

As already discussed above, the CDW energy gap could be identified from the peak position of the first Lorentz oscillation in the conductivity spectrum. At the lowest temperature, the Lorentz peak locates near 8500 cm^{-1} for $\text{LaTe}_{1.95}$ and 6800 cm^{-1} for $\text{CeTe}_{1.95}$, respectively. Those values are larger than the corresponding values of rare-earth tri-tellurides. Such large energy gap values would imply that the compounds are already deeply in the CDW state even at room temperature. With Se doping, CDW energy gap is reduced and the CDW order is suppressed. However, the reduction of the energy gap is small. In comparison with the undoped sample $\text{CeTe}_{1.95}$, the Lorentz peak, which locates at 6000 cm^{-1} , is shifted by only 800 cm^{-1} for $\text{CeTe}_{1.79}\text{Se}_{0.16}$ sample. Even if we assume that the ratio of the $2\Delta/k_B T_c \approx 8$, a number higher than BCS value but still often seen in strongly coupling materials¹⁷, we expect

that the CDW transition temperature would be still higher than 1000 K. In reality, the CDW transition temperature appears at 345 K. To our knowledge, the CDW transition temperature close to room temperature in the RTe_2 system has never been observed before. Our study suggests that, in the heavily disordered system, the ratio of the CDW energy gap over the transition temperature does not follow the value as normally expected from the BCS mean-field theory for density wave instability. Compared with the undoped samples, the peak structure becomes much weaker. Our observations seem to indicate that the disorder or localization effect arising from Te vacancies or Se substitutions affects the the CDW transition temperature more radically than the energy gap. We also emphasize that our results are strongly against the conclusions drawn by Garcia *et al.* based on ARPES study that CDW gap size decreases dramatically as the number of the Te layers reduces from two (RTe_3) to one (RTe_2) and the RTe_2 would be examples of semiconducting quasi-2D CDW material due to the gapping of the entire Fermi surfaces.

IV. CONCLUSIONS

To conclude, we have performed an optical study on the single-crystals of $\text{LaTe}_{1.95}$, $\text{CeTe}_{1.95}$ and $\text{CeTe}_{1.79}\text{Se}_{0.16}$, belonging to the layered quasi-two-dimensional charge density wave systems. Our measurement revealed clearly the formation of partial energy gaps at rather high energy levels: $2\Delta \sim 8500 \text{ cm}^{-1}$ ($\sim 1.06 \text{ eV}$) for $\text{LaTe}_{1.95}$, and 6800 cm^{-1} ($\sim 0.84 \text{ eV}$) for $\text{CeTe}_{1.95}$. A small fraction of Se substitutions for Te dramatically weaken the CDW order and suppress the phase transition temperature. As a result, the CDW phase transition was observed, for the first time, close to room temperature in the rare-earth ditelluride system. Our study also revealed that the low energy excitations of the compounds are dominantly contributed by the disorder effects due to the presence of Te vacancies in conducting Te layers. The localization modified Drude model can account for the low-frequency charge response fairly well. The spectral features are distinctly different from a semiconducting CDW state with fully gapped Fermi surfaces.

ACKNOWLEDGMENTS

This work was supported by the National Science Foundation of China (10834013, 11074291), and the 973 project of the Ministry of Science and Technology of China (2011CB921701, 2012CB821403).

¹ G. Grüner, *Density Waves in Solids* (Addison-Wesley, Reading, MA, 1994).

² E. DiMasi, B. Foran, M. C. Aronson, and S. Lee, *Chem. Mater.* **6**, 1867 (1994).

³ V. Brouet, W. L. Yang, X. J. Zhou, Z. Hussain, N. Ru, K. Y. Shin,

I. R. Fisher, and Z. X. Shen, *Phys. Rev. Lett.* **93**, 126405 (2004).

⁴ N. Ru and I. R. Fisher, *Phys. Rev. B* **73**, 033101 (2006).

⁵ E. DiMasi, M. C. Aronson, J. F. Mansfield, B. Foran, and S. Lee, *Phys. Rev. B* **52**, 14516 (1995).

⁶ Kikichi, *J. Phys. Soc. Jpn.* **67**, 1308 (1998).

- ⁷ J. H. Shim, J.-S. Kang, and B. I. Min, Phys. Rev. Lett. **93**, 156406 (2004).
- ⁸ J. Laverock, S. B. Dugdale, Zs. Major, M. A. Alam, N. Ru, I. R. Fisher, G. Santi, and E. Bruno, Phys. Rev. B **71**, 085114 (2005).
- ⁹ K. Y. Shin, V. Brouet, N. Ru, Z. X. Shen and I. R. Fisher, Phys. Rev. B **72**, 085132 (2005).
- ¹⁰ E. DiMasi, B. Foran, M. C. Aronson, S. Lee, Phys. Rev. B **54**, 13587 (1996).
- ¹¹ M. H. Jung, A. Alsmadi, H. C. Kim, Yunkyu Bang, K. H. Ahn, K. Umeo, A. H. Lacerda, H. Nakotte, H. C. Ri, and T. Takabatake, **67**, 212504 (2003).
- ¹² B. F. Hu, P. Zheng, R. H. Yuan, T. Dong, B. Cheng, Z. G. Chen, and N. L. Wang, Phys. Rev. B **83**, 155113 (2011).
- ¹³ B. F. Hu, B. Cheng, R. H. Yuan, T. Dong, A. F. Fang, W. T. Guo, Z. G. Chen, P. Zheng, Y. G. Shi, and N. L. Wang, Phys. Rev. B **84**, 155132 (2011).
- ¹⁴ D. R. Garcia, G.-H. Gweon, S. Y. Zhou, J. Graf, C. M. Jozwiak, M. H. Jung, Y. S. Kwon, and A. Lanzara, Phys. Rev. Lett. **98**, 166403 (2007).
- ¹⁵ W. B. Pearson, Zeitschrift für Kristallographie **171**, 23 (1985).
- ¹⁶ Y. S. Kwon and B. H. Min, Physica B **281C282**, 120 (2000).
- ¹⁷ W. Z. Hu, J. Dong, G. Li, Z. Li, P. Zheng, G. F. Chen, J. L. Luo, and N. L. Wang, Phys. Rev. Lett. **101**, 257005 (2008).
- ¹⁸ M. Dressel, and G. Grüner, *Electrodynamics of Solids* (Cambridge, Reading, 2002).
- ¹⁹ M. Lavagnini, A. Sacchetti, L. Degiorgi, K. Y. Shin, and I. R. Fisher, Phys. Rev. B **75**, 205113 (2007).
- ²⁰ K. E. Lee, C. I. Lee, H. J. Oh, M. A. Jung, B. H. Min, H. J. Im, T. Iizuka, Y. S. Lee, S. Kimura, and Y. S. Kwon, Phys. Rev. B **78**, 134408 (2008).
- ²¹ G. Li, P. Zheng, N. L. Wang, Y. Z. Long, Z. J. Chen, J. C. Li and M. X. Wan, J. Phys.: Condens. Matter **16** 6195 (2004).
- ²² N. F. Mott, Metal-Insulator Transitions (Taylor & Francis, London, 1990).
- ²³ R. Menon, C. O. Yoon, D. Moses, and A. J. Heeger, 1998 Handbook of Conducting Polymers 2nd ed, vol 2 (New York: Dekker).
- ²⁴ G. Tzamalís, N. A. Zaidi, C. C. Homes, and A. P. Monkman, Phys. Rev. B **66**, 085202 (2002).